THE JOURNAL OF PHYSICAL CHEMISTRY C
A JOURNAL OF THE AMERICAN CHEMICAL SOCIETY

pubs.acs.org/JPCC

Article

Reversible and Quasireversible Electron Transfer under Conditions of Differential Square-Wave Voltammetry

Dariusz Guziejewski, Leon Stojanov, Rubin Gulaboski, and Valentin Mirceski*

Cite This: *J. Phys. Chem. C* 2022, 126, 5584−5591

Read Online

ACCESS | Metrics & More | Article Recommendations

ABSTRACT: A theoretical analysis of reversible and quasireversible electrode reactions of a dissolved redox couple under conditions of the novel technique of differential square-wave voltammetry (DSWV) is presented. The technique is recently introduced as a hybrid form between differential pulse voltammetry (DPV) and square-wave voltammetry (SWV) as the two most advanced and competitive pulse-form voltammetric techniques for a purpose of unifying their advantages and further advancing both techniques in terms of analytical performances, mechanistic analysis, and electrode kinetics. The potential modulation of DSWV consists of potential steps and pulses providing a plethora of voltammetric curves, which enable in-depth characterization of the electrode reaction with a minimal set of measurements. Based on numerical simulations, a set of criteria for characterization and differentiation between reversible and quasireversible electrode reactions are established.

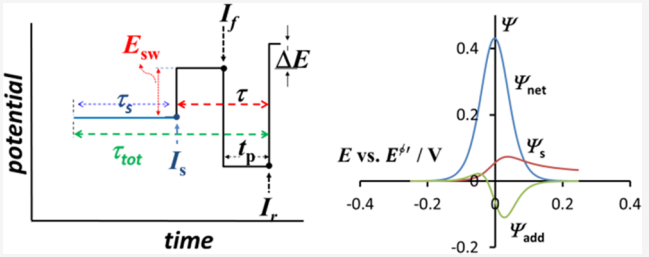

1. INTRODUCTION

The last two decades or so are highlighted with remarkable progress in voltammetry,[1,2] encompassing the advances in the theory of voltammetric techniques,[3−5] simulations of electrode mechanisms,[6−8] kinetics of electrode processes,[9−13] and the novel type of pulse voltammetric techniques.[14] Pulse voltammetry is of distinct importance in the broad area of electroanalysis; moreover, pulse techniques are exceptionally important for studying electrode kinetics[15−17] and they aided significantly in voltammetric studies of electron-transfer theories.[18−20] The family of pulse voltammetric techniques has been constantly expanding with new techniques exemplified with differential double pulse voltammetry,[21] additive differential pulse voltammetry,[22] differential alternative pulse voltammetry,[23−25] and cyclic multipulse voltammetry[26] to mention just a few. Frequently, pulse techniques have been applied in a reverse mode[27,28] or in a cyclic fashion,[29−31] intending to unify their inherent advantages with conventional cyclic voltammetry. In the context of conventional cyclic voltammetry, as an inevitable technique in any electrochemical study, we do also witness a significant progress in the studies with nontriangular waveforms of Compton et al. aiming to circumvent the inherent drawbacks related to the charging current.[32,33] Moreover, the latter methodology introduces the concept of a single voltammetry experiment conducted with a range of scan rates, which might be an exciting direction for further advancing voltammetry in general. Accordingly, we have recently proposed a multifrequency approach in a single experiment under conditions of electrochemical faradic spectroscopy,[34] which finds some analogy with a multiscan rate analysis in the method of Compton et al.[33] Electrochemical faradic spectroscopy,[35] as a simple square-wave chronoamperometric experiment, has been derived from the conventional square-wave voltammetry (SWV)[36,37] to simplify the voltammetric analysis. It comes along with a series of new variants of SWV developed in the last decade,[29,35,38] as a quest for further advancing the technique.

In spite of the fact that SWV is one of the most advanced pulse techniques, it has been recognized that it is relatively complex; thus, simplification and further modification are worth to be considered. For instance, SW voltammetric data are less intuitively understandable compared to cyclic voltammetry, rendering SWV predominantly as a tool in electroanalysis.[39,40] In the context of electrode kinetics, SWV is superior compared to other techniques when fast, reversible, and quasireversible electrode processes are concerned; it is, however, limited when electrochemically sluggish processes are considered with a large potential separation between anodic and cathodic reactions of a single redox couple.

To advance further SWV, we have recently made an attempt to develop its differential variant termed differential square-

Received: February 18, 2022
Revised: March 7, 2022
Published: March 23, 2022

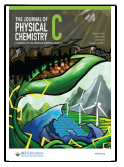

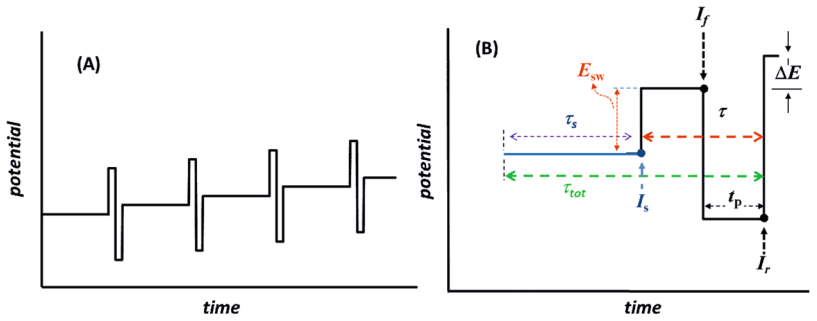

Figure 1. (A) Potential modulation and (B) one single potential cycle in differential square-wave voltammetry. Panel B shows critical parameters of the potential modulation together with the current sampling points.

wave voltammetry (DSWV),[41] proposing a new potential modulation that is more appropriate for kinetic analysis of both fast and sluggish electrode processes while keeping the ability to study the electrode mechanism; in addition, the technique has a promising analytical performance being able to improve the response with respect to the background current discrimination in comparison with conventional SWV.

The potential modulation of DSWV, depicted in Figure 1A, consists of a train of potential steps combined with potential pulses. A potential cycle of duration τ_{tot} consists of a step potential (τ_s) followed by two, equal in heights, oppositely oriented potential pulses with duration t_p (Figure 1B); thus, $\tau_{tot} = \tau_s + 2t_p$. The inverse value of $2t_p$ is known as the SW frequency f ($f = 1/(2t_p)$). Commonly, t_p ranges from 0.5 to 100 ms. In analogy to differential pulse voltammetry, the technique is characterized by a step-to-pulse duration ratio $r = \tau_s/t_p$, which together with the SW frequency is a critical parameter of the technique.

By measuring the current before the application of the pulses (I_s in Figure 1B), as well as at the end of each pulse (I_f and I_r in Figure 1B), both SW forward (I_f) and reverse (I_r) voltammetric components can be transformed into differential curves, designated as $I_{f,diff} = I_f - I_s$ and $I_{r,diff} = I_r - I_s$, respectively. By analogy to SWV, the net, differential voltammetric component can be constructed as well ($I_{net} = I_f - I_r$). Finally, as proposed by Molina,[22] an additive component can be constructed, i.e., $I_{add} = I_{f,diff} + I_{r,diff} = I_f + I_r - 2I_s$. Thus, the voltammetric response can be represented by seven components, which provides a broad basis for in-depth electrochemical characterization.

Following the first introductory study,[41] in the current communication, fundamental voltammetric characteristics of both reversible and quasireversible electrode reactions of a dissolved redox couple at a planar electrode are elucidated by means of numerical simulations. Theoretical predictions are partly illustrated by experiments conducted with the $[Fe(CN)_6]^{4-}/[Fe(CN)_6]^{3-}$ redox couple at a platinum electrode (Pt) as a model for a fast electrode reaction of a dissolved redox couple.[42]

2. DETAILS ON ELECTRODE MECHANISMS AND SIMULATION PROCEDURE

An electrode reaction described by eq 1 is considered. The redox couple consists of two chemically stable species dissolved in an electrolyte solution (sol), and the electrode reaction takes place at a macroscopic planar electrode

$$\mathrm{Red(sol)} \rightleftarrows \mathrm{Ox(sol)} + ne^- \tag{1}$$

For the sake of simplicity, the charge of the redox species in eq 1 is omitted. At the beginning of the experiment, only Red species are present in the solution at a bulk concentration of c^*, and the diffusion coefficient (D) of both Red and Ox is assumed to be equal. For a reversible electrode reaction, the Nernst equation holds: $c(\mathrm{Ox})_{x=0} = c(\mathrm{Red})_{x=0} \exp(\phi)$, where $\phi = \frac{nF}{RT}(E - E^{\phi'})$ is a dimensionless electrode potential defined versus the formal potential of the redox couple ($E^{\phi'}$). For a quasireversible case, one-electron reaction is assumed ($n = 1$) and the electrode kinetics is described with a Butler–Volmer kinetic model, i.e., $\frac{I}{FA} = k_s \exp(\alpha\phi)[(c_{Red})_{x=0} - (c_{Ox})_{x=0}\exp(-\phi)]$; it is attributed with the standard rate constant k_s (cm s^{-1}), anodic electron-transfer coefficient α, where the dimensionless potential is simplified to $\phi = \frac{F}{RT}(E - E^{\phi'})$. Following eqs 2 and 3 were applied for numerical simulations of a reversible and quasireversible electrode reaction, respectively, which were derived following the step function method[43]

$$\psi_m = \frac{\sqrt{50\pi}}{2}\frac{\exp(\phi_m)}{1 + \exp(\phi_m)} - \sum_{j=1}^{m-1} \psi_j S_{m-j+1} \tag{2}$$

$$\psi_m = \frac{\kappa \exp(\alpha\phi_m)\left\{1 - \frac{2[1 + \exp(-\alpha\phi_m)]}{\sqrt{50\pi}} \sum_{j=1}^{m-1} \psi_j S_{m-j+1}\right\}}{1 + \frac{2\kappa \exp(\alpha\phi_m)}{\sqrt{50\pi}}[1 + \exp(-\phi_m)]} \tag{3}$$

The dimensionless current is defined as $\psi = \frac{I}{nFAc^*\sqrt{Df}}$, A is the electrode surface area, $S_m = \sqrt{m} - \sqrt{m-1}$ is the numerical integration parameter, and m is the serial number of time increments. The time increment is $d = \frac{1}{50f}$, which means that each potential pulse is divided into 25 equal increments. Accordingly, the number of time increments for the potential step τ_s is $25r$, where $r = \tau_s/t_p$ is the step-to-pulse duration ratio. In addition, $\kappa = \frac{k_s}{\sqrt{Df}}$ is the electrode kinetic parameter, and other symbols have their common meaning.

3. EXPERIMENTAL SECTION

All chemicals used were of analytical grade purity (Sigma-Aldrich, ChemLab or POCh). Aqueous solutions were prepared with deionized water with the Millipore Direct Q-3 (Merck) purification system. Stock solutions of $K_4[Fe(CN)_6]$, $K_3[Fe(CN)_6]$, and KNO_3 were prepared in water. In all experiments, the electrolytic cell contained an equimolar

https://doi.org/10.1021/acs.jpcc.2c01188
J. Phys. Chem. C 2022, 126, 5584−5591

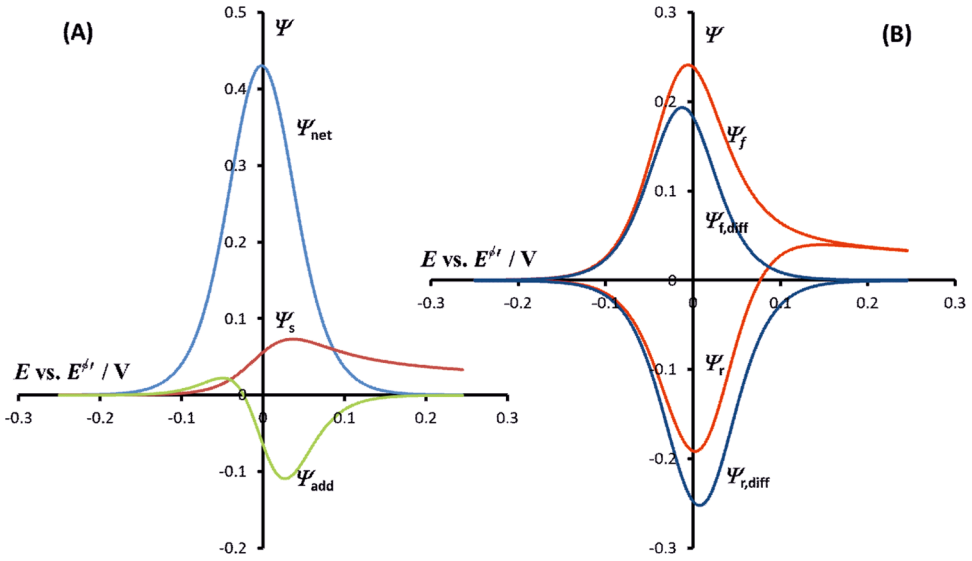

Figure 2. Reversible electrode reaction. Typical response showing all voltammetric components for the step-to-pulse ratio $r = 10$. Panel (A) depicts the net component (Ψ_{net}), the step component (Ψ_s), and the additive component (Ψ_{add}), while panel (B) displays the square-wave forward (Ψ_f) and reverse (Ψ_r) components and the differential forward ($\Psi_{f,diff}$) and reverse ($\Psi_{r,diff}$) components. The conditions of the simulations are temperature $T = 298.15$ K, stoichiometric number of electrons $n = 1$, SW amplitude $E_{sw} = 25$ mV, and step potential $\Delta E = 5$ mV.

content of both forms of the redox couple at a concentration of 0.25 mmol L^{-1} in 0.1 mol L^{-1} KNO_3 used as a supporting electrolyte. All experiments were conducted at room temperature.

Experimental analysis has been performed with a multi-Autolab potentiostat model M101 (Metrohm Autolab B.V.) controlled by NOVA (v. 1.10.3) software at a Pt working electrode, combined with Ag/AgCl/3 mol L^{-1} KCl and a platinum wire as a reference and counter electrodes, respectively. As the proposed potential modulation is not provided as a ready-to-use mode in NOVA software, an appropriate protocol was designed in the frame of a multistep chronoamperometric experiment.

4. RESULTS AND DISCUSSION

4.1. Reversible Electrode Reaction. A typical dimensionless response of a reversible electrode reaction is depicted in Figure 2, revealing a wealth of electrochemical data collected in a single DSW voltammetric experiment. By analogy to the conventional SWV, the response consists of a net component (Ψ_{net}; Figure 2A) calculated as a difference between the SW forward (Ψ_f) and reverse (Ψ_r) currents measured at the end of the corresponding potential pulses (Figure 2B). The technique enables measuring the current at the end of the potential step (τ_s) as well, thus resulting in the step component Ψ_s, which finds its analogy to the simple staircase voltammetry[44] (Figure 2A). The most typical voltammetric curves of the technique are the differential forward ($\Psi_{f,diff} = \Psi_f - \Psi_s$) and reverse ($\Psi_{r,diff} = \Psi_r - \Psi_s$) components, calculated as a difference between the current at the end of the corresponding pulse and the step potential, following the methodology typical for differential pulse voltammetry (DPV)[45] (Figure 2B). Note that the net component can also be defined as $\Psi_{net} = \Psi_{f,diff} - \Psi_{r,diff}$. Finally, an additive voltammetric component can be constructed $\Psi_{add} = \Psi_{f,diff} + \Psi_{r,diff} = \Psi_f + \Psi_r - 2\Psi_s$, which could be understood as a primitive derivation of the net voltammetric curve for a purpose of its advanced morphological characterization[14] (Figure 2A).

As in SWV,[46] the dimensionless net peak-current ($\Psi_{net,p}$) is independent of the frequency; thus, the real net peak-current ($I_{net,p}$) depends linearly on $\sqrt{f}$ for a given value of the step-to-pulse ratio (r). In other words, the ratio $I_{net,p}/\sqrt{f}$ is a constant for a reversible electrode reaction. An increase of the ratio r by extending the step duration τ_s for a given frequency has a negligible effect on the $\Psi_{net,p}$ over the interval $r \leq 40$. Thus, taking into account the current normalization, the real net peak-current can be expressed as $I_{net,p} = (0.431 \pm 0.001)nFAc^*\sqrt{Df}$ for $r \leq 40$ and conditions valid for Figure 2. The latter indicates that analytical performances of the technique are not sacrificed by increasing the duration of the potential steps for the purpose of optimizing the voltammetric response for analytical application. On the contrary, the extension of τ_s is expected to be beneficial for discriminating against the background parasitic current, thus improving the analytical performances.

The net peak-potential (E_p) and the half-peak width are independent of the frequency, identical as in conventional SWV,[46] whereas forward (Ψ_f) and reverse (Ψ_r) components gain a more pronounced peak-like shape than in SWV (cf. Figure 2B). It is a consequence of the overall scan rate decreasing in DSWV $\left(v = \frac{2f\Delta E}{r+2}\right)$ in comparison to SWV ($v = f\Delta E$)[47] for an identical frequency, causing expansion of the diffusion layer thickness in the course of the DSWV experiment. The relative position of Ψ_f and Ψ_r, expressed as a peak-potential difference (ΔE_p), is independent of the frequency, whereas it is slightly affected by increasing r; e.g., $\Delta E_p = 0$ V for $nE_{sw} = 25$ mV and $r \leq 10$.

The dimensionless peak-current of the step voltammetric component ($\Psi_{s,p}$) is also independent of the frequency for a given value of the ratio r; thus, the real peak-current is a linear function of $\sqrt{f}$. If the step-to-pulse ratio increases by extending the step potential τ_s for a constant f, the real peak-current of the step voltammetric component increases in proportion to $\tau_s^{-0.45}$, which deviates slightly from the dependence of $\tau_s^{-0.5}$, typical for the simple staircase voltammetry.[44] It is an expected

https://doi.org/10.1021/acs.jpcc.2c01188
J. Phys. Chem. C 2022, 126, 5584−5591

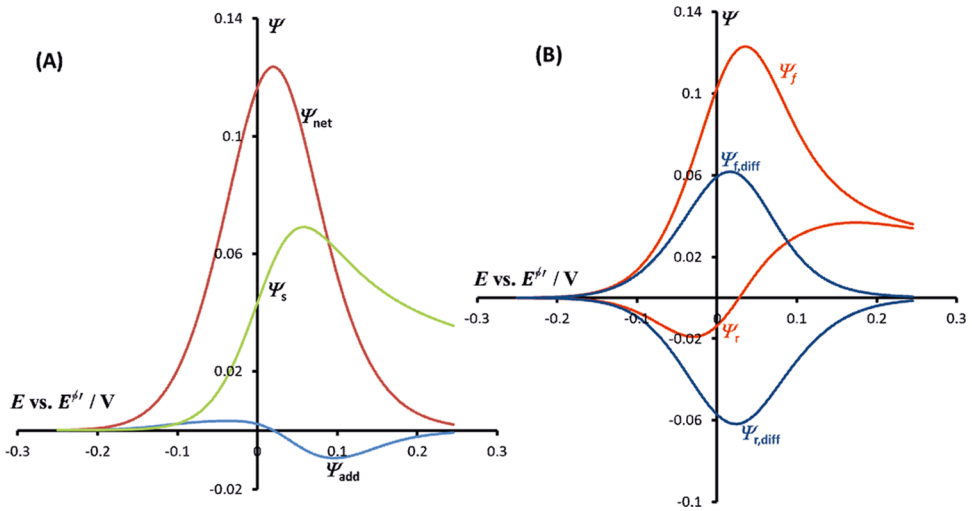

Figure 3. One-electron quasireversible electrode reaction. A typical response containing all voltammetric components for the standard rate constant $k_s = 3 \times 10^{-3}$ cm s^{-1}, electron-transfer coefficient $\alpha = 0.5$, diffusion coefficient $D = 5 \times 10^{-6}$ cm^2 s^{-1}, and SW frequency $f = 100$ Hz. The other conditions and meaning of symbols are identical as in Figure 2.

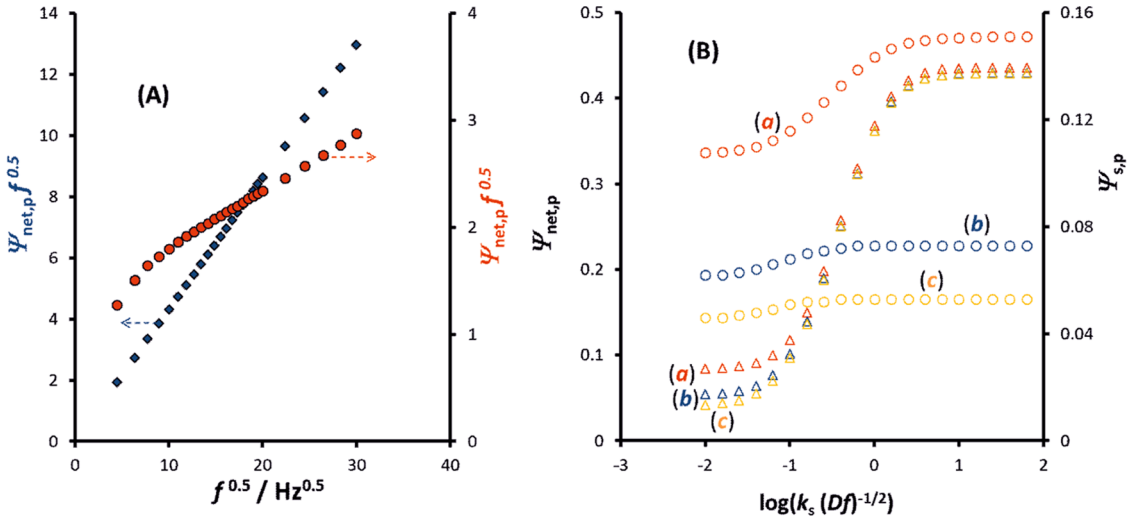

Figure 4. (A) Effect of the SW frequency on the normalized real net peak-current for a reversible (rhombuses, left ordinate) and a quasireversible (circles, right ordinate) electrode reaction, for a step-to-pulse ratio of $r = 4$ and the standard rate constant $k_s = 5 \times 10^{-3}$ cm s^{-1}. (B) The dependence of the dimensionless net peak-current (triangles, left ordinate) and the step peak-current (circles, right ordinate) on the electrode kinetic parameter for the step-to-pulse ratio $r = 2$ (*a*), 10 (*b*), and 20 (*c*). The other conditions of the simulations are identical as in Figure 3.

consequence due to the complex influence of the SW potential pulses, which separate two consecutive step potentials. The peak-potential of the step component ($E_{s,p}$) is independent of both frequency and step duration; importantly, it is separated for 35 mV from the net peak-potential for the conditions referring to Figure 2.

Differential forward ($\Psi_{f,diff}$) and reverse ($\Psi_{r,diff}$) voltammetric components are unique features of the technique, providing a new means for characterization of an electrode reaction. Both components are well-defined peaks, with readily and precisely measurable peak-current and peak-potential. Their relative relation represented by the peak-current ratio (Ψ_p(f,diff)/Ψ_p(r,diff)) and the peak-potential difference (ΔE_p(diff)) (both parameters taken in absolute values) enables us to establish new criteria for characterizing the electrode reaction. The values of Ψ_p(f,diff)/Ψ_p(r,diff) and ΔE_p(diff) are typical for a given r, being independent of the SW frequency. Importantly, differential components enable the electrode reaction to be studied at very small SW amplitudes, as they are well-defined peaks for any amplitude values over the interval $E_{sw} \geq 2$ mV. Such analysis might be advantageous in terms of the undesirable effect of both ohmic drop and charging current, which increases proportionally to the SW amplitude in SWV.[48]

The effect of the SW amplitude in the present technique could be effectively studied by inspecting the peak-potential difference of differential components. Specifically, ΔE_p(diff) vs E_{sw} is a line with a slope equal to unity and an intercept of $-\Delta E$, where ΔE is the step of the potential modulation (cf. Figure 1B). For instance, for $r = 10$ and $\Delta E = 5$ mV, the corresponding linear function over the interval $E_{sw} \leq 50$ mV reads ΔE_p(diff) (mV) = E_{sw} (mV) − 5 mV. Both the slope and the intercept of the function are independent of the SW frequency and r, as well as on the number of electrons (specifically, $n = 1$ or 2).

https://doi.org/10.1021/acs.jpcc.2c01188
J. Phys. Chem. C 2022, 126, 5584−5591

At the end of this section, it is worth mentioning that the characteristics of the additive components are very specific for given conditions and can be taken into consideration for qualitative characterization of a reversible electrode reaction (cf. Figure 2A). The morphology of the additive component is insensitive to the SW frequency, whereas it is highly susceptible to the SW amplitude and the number of electrons. The additive component is associated with the forward (Ψ_p(f,add)) and reverse (Ψ_p(r,add)) peak-current, and the potential at zero current ($E(\Psi_{add} = 0)$), i.e., the potential at the crossing point of the potential axis (cf. Figure 2A). For $r \geq 10$, the peak-current ratio is virtually independent of both time parameters f and r. In addition, the stoichiometric number of electrons can be precisely determined from the features of this voltammetric component. For instance, for simulations conducted for $r = 4$, $E_{sw} = 25$ mV, $\Delta E = 2$ mV, and $n = 1$, the forward-to-reverse peak-current ratio is 0.20 and $E(\Psi_{add} = 0) = -24$ mV vs $E^{\phi\prime}$, whereas for $n = 2$, the peak-current ratio is 0.442 and $E(\Psi_{add} = 0) = -7$ mV vs $E^{\phi\prime}$.

4.2. Quasireversible Electrode Reaction. The voltammetric response of a typical kinetically controlled electrode reaction under conditions of DSWV is depicted in Figure 3. Depending on the standard rate constant (k_s), all voltammetric curves are drifted away from the formal potential, as expected for any voltammetric technique. The relative difference between the peak-current of the net ($\Psi_{net,p}$) and the step component ($\Psi_{s,p}$) is less than for a reversible reaction (compare Figures 2A and 3A). The morphology of the forward (Ψ_f) and reverse (Ψ_r) SW components reflects the quasireversible nature of the reaction, in analogy to the conventional SWV (cf. Figure 3B).

As elaborated in our previous study,[41] the main features of the dimensionless response depend on the SW frequency, manifested through the electrode kinetic parameter $\kappa = \frac{k_s}{\sqrt{Df}}$, which controls predominantly the degree of electrochemical reversibility. In contrast to the reversible reaction, the real net peak-current ($I_{net,p}$) is a nonlinear function of $\sqrt{f}$ for a given value of the step-to-pulse ratio (Figure 4A). Over a broad range of frequencies, the ratio $\frac{I_{net,p}}{\sqrt{f}}$ is not constant, obeying a sigmoid dependence on the logarithm of $1/\sqrt{f}$. Additionally, the real peak-current of the step function depends on the SW frequency in a similar manner as the net peak-current (vide infra).

To generalize the effect of the frequency, it is recommendable to inspect the relation of the dimensionless peak-current of both net and step components as a function of the electrode kinetic parameter κ. The simulated data summarized in Figure 4B correspond to the variation of the frequency for a constant value of both r and standard rate constant k_s over the entire kinetic interval, including irreversible, quasireversible, and reversible electrochemical regions. Alternatively, the data of Figure 4B can be understood as a comparison of a series of electrode reactions associated with different standard rate constants at a given set of time parameters, thus being associated with different electrochemical reversibility. The data clearly indicate that the net component is markedly more sensitive to the electrode kinetics than the step component. When the electrochemical reversibility is estimated on the basis of the net peak-current, the data of Figure 4B imply that the electrochemical reversibility is virtually independent of r, while κ is the sole parameter controlling the reversibility. Within the typical quasireversible kinetic region (e.g., $-1.6 < \log(\kappa) < 0.8$ for conditions of Figure 4B), a narrow region exists where the ratio $I_{net,p}/\sqrt{f}$ depends linearly on $\log(1/\sqrt{f})$ (i.e., $-0.5 \leq \log(\kappa) \leq 0$), which can be used for measuring the electrode kinetics by fitting the experimental and theoretical data. Though the step peak-current follows similar sigmoid dependence on $\log(\kappa)$, it is markedly less sensitive than the net peak-current; moreover, for $r \geq 20$, it is virtually independent of the SW frequency (curve c, circles in Figure 4B).

A particularly useful approach in measuring the electrode kinetics is by inspecting the peak-current ratio of the differential components (Ψ_p(f,diff)/Ψ_p(r,diff)) by altering the SW frequency. As explained in our previous study,[41] the ratio follows a sigmoid, decreasing trend by increasing $\log(\kappa)$. Importantly, the ratio gains the value Ψ_p(f,diff)/Ψ_p(r,diff) = 1 for a given critical electrode kinetic parameter κ_c. This feature leads straightforwardly to the standard rate constant, which can be calculated as $k_s = \kappa_c\sqrt{f_c D}$, where f_c is the critical frequency determined experimentally, satisfying the condition I_p(f,diff)/I_p(r,diff) = 1. For $r > 2$, the critical value of κ_c is independent of r, whereas it depends on the SW amplitude and the electron-transfer coefficient. The critical values of κ_c increase in proportion with α. For instance, for $E_{sw} = 25$ mV, the critical values of κ_c are 0.05, 0.13, and 0.25 for α of 0.3, 0.5, and 0.7, respectively. In addition, differential components can also be exploited for estimating the electrode kinetics by altering the SW amplitude and measuring the peak-potential difference (ΔE_p(diff)). Similarly, as for the reversible electrode reaction, ΔE_p(diff) is a linear function of E_{sw} over the interval $E_{sw} \leq 50$ mV. However, for the quasireversible electrode reaction, the slope and the intercept of the line are sensitive to both electrode kinetic parameter and the electron-transfer coefficient, thus enabling the estimation of k_s and α by the fitting of the experimental and theoretical data.

Analyzing voltammetric features at a constant frequency of the pulses by increasing the step-to-pulse ratio, one finds that the ratio affects parameters of the response. For instance, for a typical quasireversible reaction attributed with $\log(\kappa) = -0.5$, the peak-potential difference (ΔE_p) between the forward and reverse SW components decreases by increasing r, opposite to the reversible reaction. If the electrochemical reversibility is estimated based on the interrelation between the differential forward and backward SW components (Ψ_p(f,diff)/Ψ_p(r,diff)), the increase of r shifts the electrode reaction toward higher electrochemical reversibility, as already discussed in our previous study.[41] Consequently, the quasireversible region of a sluggish electrode reaction is expanded by increasing r, as seen in Figure 4B (triangles; the kinetic region that is near the irreversible behavior).

For a constant frequency, within the quasireversible region, the real step peak-current decreases with $\tau_s^{-0.4}$, which is slightly different compared to the reversible reaction. At the same time, the peak-potentials of both net and step components shift toward less potentials as a consequence of a decreased scan rate, thus an enhanced electrochemical reversibility.

It is finally worth mentioning that the additive component is particularly sensitive to the electrode kinetics and can be effectively exploited for a precise estimation of the kinetic parameters.[22] Figure 5 depicts the additive component for a different degree of reversibility, showing that both peak-current ratio (Ψ_p(f,add)/Ψ_p(r,add)) and the crossing point at the potential axis ($E(\Psi_{add} = 0)$) vary significantly with the

https://doi.org/10.1021/acs.jpcc.2c01188
J. Phys. Chem. C 2022, 126, 5584−5591

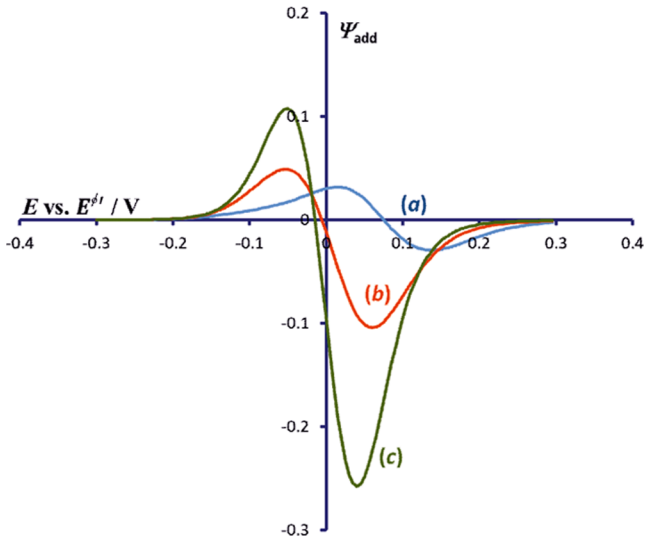

Figure 5. One-electron quasireversible electrode reaction. The additive voltammetric component simulated for different electrochemical reversibility. The electrode kinetic parameter is log (κ) = −1 (*a*), −0.5 (*b*), and 0 (*c*). The step-to-pulse ratio is r = 2, and the electron-transfer coefficient is α = 0.5. The other conditions are identical as in Figure 2.

electrode kinetic parameter. By extensive simulations under a variety of conditions (data not shown), it has been determined that the peak-current ratio is sensitive to the electrode kinetic parameter with a value up to κ = 2.5 (for r = 4); thus, assuming f = 500 Hz and $D = 5 \times 10^{-6}$ cm^2 s^{-1}, the highest measurable values of the standard rate constant can be on the order of 0.1 cm s^{-1}.

5. EXPERIMENTAL DATA

A well-defined voltammetric response of the redox couple $[Fe(CN)_6]^{3-}/[Fe(CN)_6]^{4-}$ at a platinum electrode, measured for the step-to-pulse duration ratio r = 5, and the SW frequency of f = 8, illustrates experimentally the applicability of the technique (Figure 6). In spite of the well-known complexity of the electrode reaction of hexacyanoferrates,[49−52] including the difference of the diffusion coefficients of the two redox components,[53] the features of the voltammetric response under selected experimental conditions correspond to the theoretical predictions for a fast, quasireversible electrode reaction.[42]

The richness of the voltammetric data collected in a single experiment enables the effective characterization of the studied system, which is one of the advantages of the proposed technique. For instance, analyzing the voltammetric data in Figure 6A, one finds that the crossing point at the potential axis of the additive component is $E(I_{add} = 0) = -15$ mV vs $E^{\phi\prime}$, whereas the peak-potential of the step component is $E_{s,p}$ = 40 mV vs $E^{\phi\prime}$. Here, we assume that $E^{\phi\prime}$ is identical with the net peak-potential. The peak-current ratio of the net and the step component is $I_{net,p}/I_{s,p}$ = 7.03, while the ratio of the forward and backward peaks of the additive component is I_p(f,add)/I_p(r,add)= 0.481.

Conducting simulations under corresponding conditions, by assuming a fast electrode reaction with log (κ) = 0.13 (α = 0.5 and n = 1),[46] one finds that $E(\Psi_{add} = 0) = -15$ mV vs $E^{\phi\prime}$ and $E_{s,p}$ = 40 mV vs $E^{\phi\prime}$, whereas the peak-current ratios are $\Psi_{net,p}/\Psi_{s,p}$ = 7.61 and Ψ_p(f,add)/Ψ_p(r,add) = 0.484, which is in excellent agreement with the experimental data. Let us note that if the simulations are done with the stoichiometric number of electrons n = 2, the ratio is Ψ_p(f,add)/Ψ_p(r,add)= 0.651, which does not correspond to the experimental value. Hence, as indicated in the theoretical part, the ratio Ψ_p(f,add)/Ψ_p(r,add) can be effectively exploited for the estimation of the number of electrons in the electrode equation.

Referring to the forward and backward components presented in Figure 6B, the peak-potential separation (ΔE_p) of the SW components is close to 25 mV, while the differential components are separated for 45 mV (ΔE_p(diff)). The peak-current ratio of the differential components is I_p(f,diff)/I_p(r,diff) = 0.872. Theoretical data simulated for log (κ) = 0.13 are associated with the potential separation of 30 and 45 mV for the SW and differential components, respectively, whereas the peak-current ratio is Ψ_p(f,diff)/Ψ_p(r,diff) = 0.810.

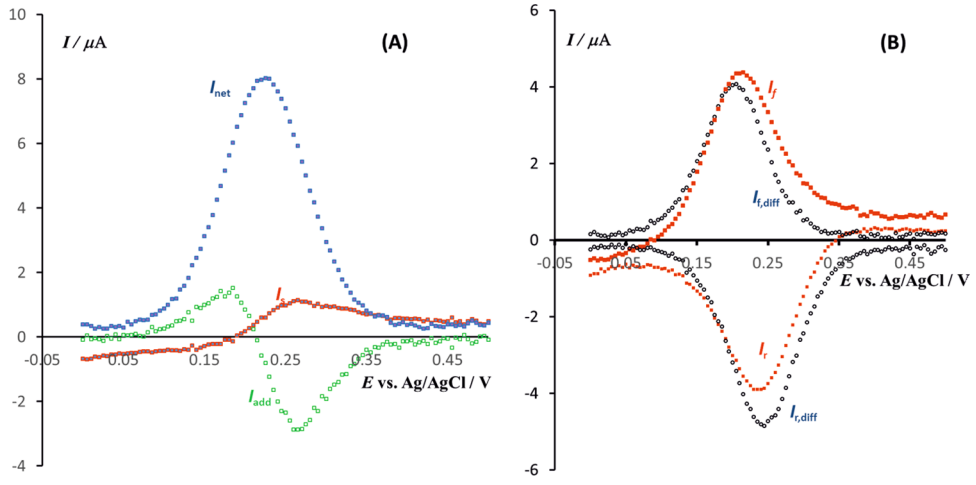

Figure 6. Typical experimental voltammetric response under conditions of DSWV of $[Fe(CN)_6]^{4-}/[Fe(CN)_6]^{3-}$ at an equimolar bulk concentration of both components of the redox couple of 0.25 mmol L^{-1}, recorded in 0.100 mol L^{-1} aqueous solution of KNO_3 at the Pt electrode. Panel (A) depicts the net (I_{net}), the step (I_s), and the additive (I_{add}) voltammetric components, while panel (B) displays the square-wave forward (I_f) and reverse (I_r) components, and the differential forward ($I_{f,diff}$) and reverse ($I_{r,diff}$) components. The step-to-pulse ratio is r = 5. Other parameters of the potential modulation are f = 8 Hz, E_{sw} = 50 mV, and ΔE = 5 mV.

https://doi.org/10.1021/acs.jpcc.2c01188
J. Phys. Chem. C 2022, 126, 5584−5591

Further experimental analysis has been done by changing the step-to-pulse duration ratio r within the interval from 1 to 25 for a constant SW frequency of f = 8 Hz. As predicted by the theory for a reversible or fast electrode reaction, the peak-potential of both net and step components remained unaffected by r. The net peak-current slightly varied with r, with an average value of $I_{net,p}$ = (7.78 ± 0.23) μA, whereas the peak-current of the step component is a linear function of $r^{-0.45}$ (R^2 = 0.999), which is in excellent agreement with the theoretical predictions. The peak-current ratio of the differential forward and reverse components increases from 0.73 to 0.85 for r = 1 and 25, respectively; the same trend holds for the peak-current ratio of the additive component.

Finally, the effect of the SW amplitude was studied for three values of r (i.e., r = 1, 5, and 10) and the peak-potential separation (ΔE_p(diff)) of the differential forward and backward components was measured as a function of E_{sw}, over the amplitude interval from 5 to 50 mV. Generally, the relationship ΔE_p(diff) vs E_{sw} does not depend on r, as predicted by the simulations for a reversible reaction. The best linearity was found for r = 5, and the regression line is ΔE_p(diff)= 0.967E_{sw} + 4.70 (R^2 = 0.905), where all values are expressed in millivolts. These experimental data are in accord with the theory in which it was predicted that the slope of the latter function is 1, while the intercept is equal to the step potential increment (i.e., 5 mV in the present experiment).

6. CONCLUSIONS

Differential square-wave voltammetry is a novel, hybrid technique between conventional differential pulse and square-wave voltammetry, which is designed to unify the advantages of both techniques, in terms of analytical sensitivity and mechanistic and kinetic characterization of both very fast and sluggish electrode processes. A single voltammogram consists of seven voltammetric curves; hence, a plethora of voltammetric parameters can be measured (i.e., peak-currents and peak-potentials), in addition to the interrelation between these parameters (i.e., peak-current ratios and peak-potential differences), providing a basis for the effective and in-depth characterization of the studied electrode reaction in a fast and effective procedure. In addition, the additive voltammetric component provides a new means for the estimation of the number of electrons in the electrode reaction equation, electron-transfer coefficient, and the standard rate constant, extending the kinetic interval up to the rate constants of 0.1 cm s^{-1}. The nature of differential and additive voltammetric components does not require background correction in the experimental analysis, thus providing voltammetric data of superior quality, which leads to a reliable kinetic characterization as well as promising advanced analytical application of the technique.

AUTHOR INFORMATION

Corresponding Author

Valentin Mirceski − *Department of Inorganic and Analytical Chemistry, University of Lodz, 91-403 Lodz, Poland; Institute of Chemistry, Faculty of Natural Sciences and Mathematics, Ss Cyril and Methodius University in Skopje, 1000 Skopje, R. North Macedonia;* orcid.org/0000-0002-9191-3926; Email: valentin@pmf.ukim.mk

Authors

Dariusz Guziejewski − *Department of Inorganic and Analytical Chemistry, University of Lodz, 91-403 Lodz, Poland;* orcid.org/0000-0002-0990-321X

Leon Stojanov − *Institute of Chemistry, Faculty of Natural Sciences and Mathematics, Ss Cyril and Methodius University in Skopje, 1000 Skopje, R. North Macedonia*

Rubin Gulaboski − *Faculty of Medical Sciences, Goce Delcev University - Stip, 2000 Stip, R. North Macedonia*

Complete contact information is available at: https://pubs.acs.org/10.1021/acs.jpcc.2c01188

Notes

The authors declare no competing financial interest.

ACKNOWLEDGMENTS

V.M. and D.G. are grateful for the support of the Opus Lap grant no. 2020/39/I/ST4/01854 by the National Science Centre of Poland. R.G. thanks Alexander von Humboldt foundation (Germany) for the support in 2021.

REFERENCES

(1) Batchelor-McAuley, C.; Kätelhön, E.; Barnes, E. O.; Compton, R. G.; Laborda, E.; Molina, A. Recent advances in voltammetry. *ChemistryOpen* **2015**, *4*, 224−260.

(2) Laborda, E.; González, J.; Molina, Á. Recent advances on the theory of pulse techniques: A mini review. *Electrochem. Commun.* **2014**, *43*, 25−30.

(3) Laborda, E.; Martínez-Ortiz, F.; Molina, Á. Study of electrochemical processes with coupled homogeneous chemical reaction in differential pulse voltammetry at spherical electrodes and microhemispheres. *Electroanalysis* **2010**, *22*, 1857−1866.

(4) Molina, A.; González, J.; Laborda, E.; Wang, Y.; Compton, R. G. Catalytic mechanism in cyclic voltammetry at disc electrodes: An analytical solution. *Phys. Chem. Chem. Phys.* **2011**, *13*, 14694−14704.

(5) Molina, A.; Gonzalez, J.; Laborda, E.; Li, Q.; Batchelor-McAuley, C.; Compton, R. G. Electrochemical behavior of two-electron redox processes by differential pulse techniques at microelectrodes. *J. Phys. Chem. C* **2012**, *116*, 1070−1079.

(6) Rudolph, M. Digital simulation with the fast implicit finite difference (FIFD) algorithm: Part 5: Digital simulations of square wave voltammetry for any user defined electrochemical mechanism comprising first- and second-order chemical reactions. *J. Electroanal. Chem.* **2001**, *503*, 15−27.

(7) Dickinson, E. J. F.; Ekström, H.; Fontes, E. COMSOL Multiphysics: Finite element software for electrochemical analysis. A mini-review. *Electrochem. Commun.* **2014**, *40*, 71−74.

(8) Britz, D.; Strutwolf, J. *Digital Simulation in Electrochemistry*, 4th ed., Scholz, F., Ed.; Springer: Cham, 2016.

(9) Mirčeski, V.; Lovrić, M. Split square-wave voltammograms of surface redox reactions. *Electroanalysis* **1997**, *9*, 1283−1287.

(10) Mirceski, V.; Guziejewski, D.; Lisichkov, K. Electrode kinetic measurements with square-wave voltammetry at a constant scan rate. *Electrochim. Acta* **2013**, *114*, 667−673.

(11) Guziejewski, D.; Mirceski, V.; Jadresko, D. Measuring the electrode kinetics of surface confined electrode reactions at a constant scan rate. *Electroanalysis* **2015**, *27*, 67−73.

(12) Mirceski, V.; Smarzewska, S.; Guziejewski, D. Measuring the electrode kinetics of vitamin B2 at a constant time window of a square wave voltammetric experiment. *Electroanalysis* **2016**, *28*, 385−393.

(13) Mirceski, V.; Laborda, E.; Guziejewski, D.; Compton, R. G. New approach to electrode kinetic measurements in square-wave voltammetry: Amplitude-based quasireversible maximum. *Anal. Chem.* **2013**, *85*, 5586−5594.

(14) Molina, A.; González, J. *Pulse Voltammetry in Physical Electrochemistry and Electroanalysis: Theory and Applications*, 1st ed.; Scholz, F., Ed.; Springer: Cham, 2016.
(15) Dauphin-Ducharme, P.; Arroyo-Currás, N.; Kurnik, M.; Ortega, G.; Li, H.; Plaxco, K. W. Simulation-based approach to determining electron transfer rates using square-wave voltammetry. *Langmuir* **2017**, *33*, 4407−4413.
(16) Gulaboski, R.; Mirceski, V. New aspects of the electrochemical-catalytic (EC') mechanism in square-wave voltammetry. *Electrochim. Acta* **2015**, *167*, 219−225.
(17) Lovrić, M.; Komorsky-Lovric, Š. Square-wave voltammetry of an adsorbed reactant. *J. Electroanal. Chem.* **1988**, *248*, 239−253.
(18) Laborda, E.; Henstridge, M. C.; Molina, A.; Martínez-Ortiz, F.; Compton, R. G. A comparison of Marcus−Hush vs. Butler−Volmer electrode kinetics using potential pulse voltammetric techniques. *J. Electroanal. Chem.* **2011**, *660*, 169−177.
(19) Laborda, E.; Wang, Y.; Henstridge, M. C.; Martínez-Ortiz, F.; Molina, A.; Compton, R. G. Quantitative weaknesses of the Marcus-Hush theory of electrode kinetics revealed by reverse scan square wave voltammetry: The reduction of 2-methyl-2-nitropropane at mercury microelectrodes. *Chem. Phys. Lett.* **2011**, *512*, 133−137.
(20) Laborda, E.; Henstridge, M. C.; Compton, R. G. Asymmetric Marcus theory: Application to electrode kinetics. *J. Electroanal. Chem.* **2012**, *667*, 48−53.
(21) Molina, A.; Laborda, E.; Martínez-Ortiz, F.; Bradley, D. F.; Schiffrin, D. J.; Compton, R. G. Comparison between double pulse and multipulse differential techniques. *J. Electroanal. Chem.* **2011**, *659*, 12−24.
(22) Molina, A.; Moreno, M. M.; Serna, C.; Camacho, L. Additive differential pulse voltammetry, instead of double differential pulse voltammetry. *Electrochem. Commun.* **2001**, *3*, 324−329.
(23) Stoytcheva, M.; Zlatev, R.; Velkova, Z.; Gochev, V.; Ayala, A.; Montero, G.; Valdez, B. Resolution of a mononitrophenol isomers mixture by differential alternative pulses voltammetry. *Electroanalysis* **2019**, *31*, 652−660.
(24) Zlatev, R.; Stoytcheva, M.; Valdez, B. Application of anodic stripping differential alternative pulses voltammetry for simultaneous species quantification. *Electroanalysis* **2018**, *30*, 1902−1905.
(25) Ayala, A.; Stoytcheva, M.; Zlatev, R.; Velkova, Z.; Gochev, V.; Valdez, B.; Montero, G. Simultaneous determination of hydroquinone and catechol by differential alternative pulses voltammetry. *Electroanalysis* **2018**, *30*, 1913−1917.
(26) Jadreško, D.; Zelić, M. Cyclic multipulse voltammetric techniques. Part I: Kinetics of electrode processes. *J. Electroanal. Chem.* **2013**, *707*, 20−30.
(27) Lovrić, M.; Jadreško, D. Theory of square-wave voltammetry of quasireversible electrode reactions using an inverse scan direction. *Electrochim. Acta* **2010**, *55*, 948−951.
(28) Zelić, M.; Lovrić, M. Isopotential points in reverse square-wave voltammetry. *J. Electroanal. Chem.* **2009**, *637*, 28−32.
(29) Xinsheng, C.; Guogang, P. Cyclic square wave voltammetry: Theory and experimental. *Anal. Lett.* **1987**, *20*, 1511−1519.
(30) Helfrick, J. C., Jr.; Mann, M. A.; Bottomley, L. A. Diagnostic criteria for the characterization of electrode reactions with chemically coupled reactions preceding the electron transfer by cyclic square wave voltammetry. *ChemPhysChem* **2016**, *17*, 2596−2606.
(31) Helfrick, J. C.; Bottomley, L. A. Cyclic square wave voltammetry of single and consecutive reversible electron transfer reactions. *Anal. Chem.* **2009**, *81*, 9041−9047.
(32) Kätelhön, E.; Compton, R. G. Non-linear sweep voltammetry of adsorbed species: theory and a method to determine formal potentials. *Phys. Chem. Chem. Phys.* **2017**, *19*, 28820−28823.
(33) Uchida, Y.; Kätelhön, E.; Compton, R. G. Cyclic voltammetry with non-triangular waveforms: Electrochemically irreversible and quasi-reversible systems. *J. Electroanal. Chem.* **2018**, *810*, 135−144.
(34) Stojanov, L.; Guziejewski, D.; Puiu, M.; Bala, C.; Mirceski, V. Multi-frequency analysis in a single square-wave chronoamperometric experiment. *Electrochem. Commun.* **2021**, *124*, No. 106943.
(35) Jadreško, D.; Guziejewski, D.; Mirčeski, V. Electrochemical faradaic spectroscopy. *ChemElectroChem* **2018**, *5*, 187−194.
(36) Mirceski, V.; Gulaboski, R.; Lovric, M.; Bogeski, I.; Kappl, R.; Hoth, M. Square-wave voltammetry: A review on the recent progress. *Electroanalysis* **2013**, *25*, 2411−2422.
(37) Mirceski, V.; Gulaboski, R. Recent achievements in square-wave voltammetry (a review). *Maced. J. Chem. Chem. Eng.* **2014**, *33*, 1−12.
(38) Mirceski, V.; Stojanov, L.; Gulaboski, R. Double-sampled differential square-wave voltammetry. *J. Electroanal. Chem.* **2020**, *872*, No. 114384.
(39) Chen, A.; Shah, B. Electrochemical sensing and biosensing based on square wave voltammetry. *Anal. Methods* **2013**, *5*, 2158−2173.
(40) Castagnola, E.; Woeppel, K.; Golabchi, A.; McGuier, M.; Chodapaneedi, N.; Metro, J.; Taylor, I. M.; Cui, X. T. Electrochemical detection of exogenously administered melatonin in the brain. *Analyst* **2020**, *145*, 2612−2620.
(41) Mirceski, V.; Guziejewski, D.; Stojanov, L.; Gulaboski, R. Differential square-wave voltammetry. *Anal. Chem.* **2019**, *91*, 14904−14910.
(42) Daum, P. H.; Enke, C. G. Electrochemical kinetics of the ferri-ferrocyanide couple on platinum. *Anal. Chem.* **1969**, *41*, 653−656.
(43) Nicholson, R. S.; Olmstead, M. L. *Electrochemistry: Calculations, Simulation, and Instrumentation*; Mattson, J. S.; Mark, H. B.; MacDonald, H. C., Eds.; Marcel Dekker: New York, 1972; pp 120−137.
(44) Christie, J. H.; Lingane, P. J. Theory of staircase voltammetry. *J. Electroanal. Chem.* **1965**, *10*, 176−182.
(45) Barker, G. C.; Gardner, A. W. Pulse polarography. *Fresenius' Z. Anal. Chem.* **1960**, *173*, 79−83.
(46) Mirceski, V.; Komorsky-Lovric, S.; Lovric, M. *Square-wave Voltammetry: Theory and Application*, Scholz, F., Ed., Springer: Berlin Heidelberg, 2007.
(47) Jadreško, D.; Zelić, M.; Lovrić, M. A formal scan rate in staircase and square-wave voltammetry. *J. Electroanal. Chem.* **2010**, *645*, 103−108.
(48) Krulic, D.; Fatouros, N. Peak heights and peak widths at half-height in square wave voltammetry without and with ohmic potential drop for reversible and irreversible systems. *J. Electroanal. Chem.* **2011**, *652*, 26−31.
(49) Peter, L. M.; Dürr, W.; Bindra, P.; Gerischer, H. The influence of alkali metal cations on the rate of the Fe(CN)64−/Fe(CN)63− electrode process. *J. Electroanal. Chem.* **1976**, *71*, 31−50.
(50) Bindra, P.; Gerischer, H.; Peter, L. M. The dependence of the rate of the $Fe(CN)6^{3-}/Fe(CN)6^{4-}$ couple on ionic strength in concentrated solutions. *J. Electroanal. Chem.* **1974**, *57*, 435−438.
(51) Kim, D. Y.; Wang, J.; Yang, J.; Kim, H. W.; Swain, G. M. Electrolyte and temperature effects on the electron transfer kinetics of $Fe(CN)6^{-3/-4}$ at boron-doped diamond thin film electrodes. *J. Phys. Chem. C* **2011**, *115*, 10026−10032.
(52) Noel, M.; Anantharaman, P. N. Voltammetric studies on a glassy carbon electrode. Part II. Factors influencing the simple electron-transfer reactions—the K3[Fe(CN)6]-K4[Fe(CN)6] system. *Analyst* **1985**, *110*, 1095−1103.
(53) Konopka, S. J.; McDuffie, B. Diffusion coefficients of ferri- and ferrocyanide ions in aqueous media, using twin-electrode thin-layer electrochemistry. *Anal. Chem.* **1970**, *42*, 1741−1746.

https://doi.org/10.1021/acs.jpcc.2c01188
J. Phys. Chem. C 2022, 126, 5584−5591